EFFECT OF INITIAL FLAW SHAPES ON CRACKS EMANATING FROM FASTENER HOLES UNDER COMBINED STRESS

Pir M. Toor*

INTRODUCTION

Linear elastic fracture mechanics (LEFM) has recently been applied in predicting crack growth rates in damaged structures. The concept of crack tip stress intensity factor has been developed by Irwin [1] for a plane extrusion, symmetric with respect to the crack. Stress intensity factor has also been shown to control the growth rate of cracks when a body is subjected to cyclic loading. Despite vigorous research in linear elastic fracture mechanics, very little progress has been made for plates subjected to in-plane or out of plane bending loads.

The effort so far in bending problems has been for surface cracks. In this respect Smith, Emery and Kobayashi [2] provided an approximate solution by means of an alternating technique. Rice and Levy [3] developed an approximate solution by replacing the cracked section with a continuous spring. Grant and Sinclair [4] investigated stress intensity factors for surface cracks in bending. They replaced the surface flaw with springs and obtained a stress intensity factor where the crack border intersects the plate surface. Marrs and Smith [5] used photo-elastic techniques and obtained qualitative correlation with Smith's theory and Grant's and Sinclair's experimental data. An approximate theory for the determination of stress intensity factors under bending has also been developed by Shah and Kobayashi [6].

Most recently, Schroedl and Smith [7] investigated the local stresses near deep surface flaws under cylindrical bending fields. They compared their experimental results with various theories. Their main conclusion was that the theories were two-dimensional approximations to a complex three-dimensional problem. However, investigation and analysis of the development of early life aircraft structural failures [8] indicated that the majority of failures originated from fastener holes, corners, and surface flaws. Due to the importance of surface flaws, considerable effort has been devoted [9] to obtaining the stress intensity factors for this problem. However, due to the complexity of the stress field at the holes, very limited experimental data or empirical expressions are available for uniform uniaxial tensile loading conditions [10 - 11].

In a realistic aircraft structure, the stress conditions are often complex. Bending and tension are the primary damage contributor in the aircraft wing. To the best knowledge of the author, neither experimental nor empirical work has been done for cracks starting from fastener holes under either bending or combined bending and tensile load conditions.

The objective of this investigation was to conduct experiments for cracks emanating from fastener holes under bending and combined bending and ten-

*Lockheed-Georgia Co., Marietta, Ga. 30063, U.S.A.

sile load conditions, and from these experiments to establish empirical relations to predict the crack growth rate.

MATERIAL AND EXPERIMENTAL WORK

The material used in this investigation was 7075-T6511 extrusion. The fatigue crack growth data were obtained by using a specimen as shown in Figure 1. Various initial corner flaw geometries were incorporated and three flaw aspect ratios ao/co between .158 and 1.0 combined with two initial ao/B values between 0.125 and 0.25 resulted in six initial flaw shapes. The tests were conducted in room temperature at 90 R.H.

Initial experiments were conducted to see if axial-tension-tension fatigue loading would generate a natural crack about the entire starter flaw front prior to moving toward the natural aspect ratio for axial loaded corner flaws. The desired flaw shapes were generated using EDM process.

Four specimens were prepared representing the total range of those aspect ratios required. Fatigue cracks were then initiated. The fracture surfaces were then opened and examined. It was observed that little could be done to influence the crack front generated by the initial flaw shape. Therefore, initial flaw shapes were developed by three different methods. For ao/co = 1.0, the initial flaw shape was developed under tension-tension cycling. For ao/co = 0.5, the initial flaw shape was generated under pure bending conditions. Finally, for ao/co = .25, the specimen was designed oversize in width and thickness, the initial shape was developed and then the specimen was machined to the standard size of Figure 1. Three specimens were used to check the accuracy of the flaw shape for the last case. Before generating the fatigue crack, both the hole wall and the surface adjacent to the hole were polished to enhance visibility of the crack front.

TEST PROCEDURE

All tests were conducted in a 133 kN capacity MTS closed loop testing system. All tests were conducted at a stress ratio of 0.1 and a cyclic rate of 10 hertz. Tension experiments were conducted with fixed grips on the machine, while the combined bending and tension test set up was identical to the tension set up with two exceptions. The universal grips were placed on both loading forks and the specimen was installed off-centre with washers, as shown in Figure 2. Bending tests were done under three-point loading. Axial strain gages were then placed on each specimen on the vertical centreline 6.35 mm above the hole. The desired strain distribution was achieved by shifting the specimens off centre using washers.

Crack growth readings were taken using high intensity light and a 30-power binocular microsope. During testing the machine was stopped periodically, the positions of the crack tip in the hole wall and on the outer surface were marked, using a specially designed scribe, and the number of cycles was recorded. After testing, each specimen was sectioned and the distance to each scribe mark from the hole wall edge was measured using a microscope.

RESULTS AND DISCUSSION

The results of the fatigue crack growth experiments were presented in

Table 1 through 3, for tension, bending, and combined tension and bending respectively. The tables give the values of a and c at given increments in the number of cycles applied.

The fatigue crack growth data were analyzed using a stress intensity concept. It was assumed that cracks propagated under conditions of plain strain and at the location of maximum stress intensity. In general a stress intensity expression in terms of important parameters affecting the crack extension can be written as:

$$K = \sigma\sqrt{\pi a}\ \beta_f \beta_b \cdot \beta_w \cdot \beta_h \cdot M/\phi \qquad (1)$$

where β_f is a factor accounting for the influence of the front free surface, i.e., the surface coincident with the visible length of the crack; β_b a factor accounting for the back surface of the specimen. In this analysis Kobayashi's [12] back surface correction factor is used. β_h is the factor accounting for the influence of the hole, the Bowie [13] correction factor. β_w is the width correction factor, secant correction. The other symbols have the standard definition. When a = c, i.e., for a circular crack, M approaches unity and ϕ becomes $\pi/2$. When a ≠ c, the flaw shape deviates from quarter circular and some modification to the above equation must be applied to account for the shape change.

One of the empirical analysis approaches for the stress intensity factors for truncated elliptical cracks is given in reference [14]. It is the author's experience that this analysis is too laborious for general use. Instead it was thought appropriate to use the simple quick analysis approach outlined in reference [10]. Here the stress intensity factor is written in terms of equivalent crack length as:

$$K = C\ \sigma\sqrt{\pi c_e}\ \beta(c_e/r) \cdot \beta_b \cdot \beta_f \qquad (2)$$

where c_e is the equivalent crack length, $\beta(c_e/r)$ is the Bowie function for an equivalent crack, the other symbols are defined previously. A plot for c_e/c versus a/B for various a/c values is given in reference [10] Figure 31. This data will be referred to as variable flaw data. for any shape a/c interpolation can be made for analysis purposes. These values were used with Bowie's correction factor. It has been suggested [10] that c_e/c were found to relate to a/c and a/B for a value of C = 0.87.

The present analysis was carried out using equation (2) with appropriate correction factors. Fatigue crack growth predictions were made using Paris' equation [15] given below:

$$da/dN = C(\Delta K)^n \qquad (3)$$

Analysis was carried out, using the maximum stress, irrespective of the type of loading, i.e., tension, bending or combined tension and bending. The correction for type of loading was made in the beta factors. The general trend of the experimental data was that under pure bending the crack growth was slower than combined bending and tension, which in turn was slower than pure tension. This trend was consistent for all initial a/c ratios. An interesting observation was that the surface crack c did

not start propagating for a/c in the range of .158 to .193 in the three types of loading until the ratio had reached about .4 to .63.

The analysis showed that using the Bowie correction for a single edge crack with appropriate variable flaw data gave an excellent correlation, as shown in Figure 3. Using only Bowie's solution gave a much shorter life for tension testing. For bending, and combined bending and tension the correlation was reasonable, as shown in Figure 4. It must be pointed out here that the effect of the hole wall on crack growth under the last two types of testing was much more pronounced. Further study is under way to separate this parameter based on a specific crack shape parameter.

CONCLUSIONS

- From this investigation it can be concluded that for pure tension Bowie and variable flaw data factors give excellent results and the method can be used with confidence.

- For bending, and combined bending and tension the correlation is reasonable, but needs further study before using it with confidence.

ACKNOWLEDGEMENT

This work was carried out at Lockheed-Georgia Company. The author wishes to express his gratitude to A. P. Shewmaker, S. C. Rogers and N. C. Appold for their encouragement throughout the work. Acknowledgement is due to Wade McGee and Ron Michael of Department 72-61 for conducting the experiments.

REFERENCES

1. IRWIN, G. R., Journal of Applied Mechanics, 29, 4, Trans. ASME, Series E, 1962, 651.
2. SMITH, F. W., EMERY, A. F. and KOBAYASHI, A. S., Trans. ASME, Series E, 89, 1967, 953.
3. RICE, J. R. and LEVY, N., Tech. Report, Div. of Engr. Brown University, Providence, R.I., September 1970.
4. GRANT, A. F. and SINCLAIR, G. M., ASTM-STP-513, Part 1, 1971, 37.
5. MARRS, G. R. and SMITH, C. V., ASTM-STP-513, Part I, 1971, 22.
6. SHAH, R. C. and KOBAYASHI, A. S., ASTM-STP-513, Part I, 1971, 23.
7. SCHROEDL, M. A. and SMITH, C. W., ASTM-STP-536, 1973, 45.
8. GRAN, R. J., ORAZIO, F. D., PARIS, P. C., IRWIN, G. R. and HERTZBERG, R., AFFDL-TR-70-1439, Wright-Patterson Air Force Base, Ohio, 1971.
9. GRANT, A. F. and GALLAGHER, J. P., ASTM-STP-560, Part I.
10. HALL, R. and FINGER, R. W., AFFDL-TR-70-144-70, Wright-Patterson Air Force Base, Ohio, 1970, 235.
11. SHAH, R. C., 8th National Symposium on Fracture Mechanics, Brown University, Providence, R.I., August 1974.
12. KOBAYASHI, A. S. and SHAH, R. C., ASME, 1972, 79.
13. BOWIE, O. L., J. of Math. and Phys., 23, 1, April 1956, 60.
14. HSU, T. M. and LIU, A. F., 7th National Symposium on Fracture Mechanics, University of Maryland, August 1973.
15. PARIS, P. C. and ERDOGAN, F., Journal of Basic Engineering, December 1963, 528.

Table 1 Flaw Growth Data Under Tension R = 0.1, σ_{max} = 103 MPa

Specimen EL-1 ao = 1.8 co = 1.8			Specimen BR-1 ao = 3.1 co = 3.2			Specimen CL-1 ao = 1.9 co = 3.1			Specimen CR-1 ao = 3.5 co = 5.9			Specimen TL-1 ao = 1.3 co = 6.9			Specimen TR-1 ao = 2.1 co = 13.5		
N	a	c	N	a	c	N	a	c	N	a	c	N	a	c	N	a	c
2500	2.5	2.5	2000	3.7	3.5	2000	2.4	3.3	2000	4.7	6.2	2000	2.1	6.9	1000	2.5	13.5
2500	3.3	2.5	3000	4.8	3.8	2000	3.2	3.5	2000	5.7	6.7	2000	3.1	6.9	1000	3.1	13.5
2500	4.2	3.2	2500	5.7	4.3	2000	3.9	3.9	2000	7.1	7.5	2000	4.3	6.9	1000	3.8	13.5
2500	5.4	3.9	2500	6.7	4.9	2000	4.7	4.5	2000	8.4	8.6	2000	5.6	7.1	1000	4.3	13.5
2500	6.6	4.8	2500	7.7	5.5	2000	6.0	5.1	2000	9.6	9.9	2000	7.0	8.0	1000	5.0	13.5
2500	7.8	5.8	2500	8.7	6.4	2000	7.1	5.9	2000	11.3	11.6	2000	8.5	9.0	1000	5.6	13.5
2500	8.9	7.1	2500	9.7	7.2	2000	8.1	6.9	500	12.7	12.3	2000	9.3	10.2	1000	6.4	13.9
2000	10.6	8.6	2500	11.0	8.2	2000	9.4	7.9				2000	11.0	11.3	1000	7.0	14.3
2000	11.7	10.1	2850	12.7	9.5	2000	10.7	9.3				1800	12.7	13.5	1000	7.7	14.6
2000	12.7	10.9				1500	11.8	10.5							1000	8.5	15.0
															1000	9.3	15.5
															1000	10.0	16.2
															1000	10.5	17.2
															1000	11.4	18.2

NOTE: All crack lengths are in mm.
All tests were terminated when "a" reached near surface of specimen.

Table 2 Flaw Growth Data Under Bending R = 0.1, σ_{max} = 103 MPa

Specimen BL-2 ao = 1.5 co = 1.73			Specimen BR-2 ao = 3.1 co = 3.2			Specimen CL-2 ao = 1.8 co = 3.0			Specimen CR-2 ao = 3.5 co = 6.0			Specimen TL-2 ao = 1.2 co = 6.8			Specimen TL-2 ao = 2.2 co = 13.4		
N	a	c	N	a	c	N	a	c	N	a	c	N	a	c	N	a	c
10,000	1.73	1.9	30,000	3.1	3.2	10,000	2.2	3.0	20,000	3.8	6.7	7,500	2.8	6.8	5,000	2.7	13.4
10,000	2.1	2.2	30,000	3.1	3.5	10,000	2.5	3.2	30,000	4.1	7.8	7,500	2.8	6.8	5,000	3.4	13.4
20,000	2.4	2.8	60,000	3.1	4.1	20,000	2.8	3.5	30,000	4.4	9.3	7,500	3.5	6.8	5,000	4.0	13.4
30,000	2.8	3.7	30,000	3.1	4.5	20,000	3.0	3.8	30,000	4.6	10.8	7,500	4.0	6.8	5,000	4.5	13.4
25,000	3.4	4.4	30,000	3.1	4.9	20,000	3.2	4.2	30,000	4.8	12.3	10,000	4.2	6.8	10,000	5.0	13.4
30,000	3.8	5.7	30,000	3.9	5.8	20,000	3.5	4.7	30,000	5.1	14.0	10,000	4.4	7.6	10,000	5.4	14.0
30,000	4.3	7.2	30,000	4.3	7.2	20,000	3.7	5.2	30,000	5.4	16.5	10,000	4.7	8.3	10,000	5.4	14.9
30,000	4.7	8.4	30,000	4.8	9.1	30,000	3.9	5.9	30,000	5.7	20.4	10,000	4.7	9.1	10,000	5.4	15.9
30,000	4.7	9.0	30,000	5.1	11.3	30,000	4.1	6.8				10,000	4.7	10.1	10,000	5.4	16.8
30,000	4.7	12.0	30,000	5.5	14.7	30,000	4.4	8.1				10,000	4.7	11.0	10,000	5.4	18.1
						30,000	4.5	9.8									
						30,000	4.5	11.6									
						30,000	4.5	13.6									

NOTE: All crack lengths are in mm.
All tests were terminated when "a" reached near surface of specimen.

Table 3 Flaw Growth Data Under Combined Bending and Tension R = 0.1, σ_{max} = 103 MPa

Specimen BL-3 ao = 1.7 co = 1.4			Specimen BR-3 ao = 3.3 co = 3.1			Specimen CL-3 ao = 2.0 co = 3.1			Specimen DR-3 ao = 3.7 co = 6.2			Specimen TL-3 ao = 1.3 co = 6.7			Specimen TL-3 ao = 2.2 co = 13.4		
N	a	c	N	a	c	N	a	c	N	a	c	N	a	c	N	a	c
3000	2.3	1.4	2000	3.5	3.2	2000	2.5	3.3	2000	4.6	6.6	3000	2.1	6.7	2000	3.0	13.4
3000	3.2	2.7	1000	3.9	3.4	2000	3.1	3.5	2000	5.3	7.0	3000	3.1	6.7	3000	4.5	13.4
3000	4.0	3.2	2000	4.5	3.6	2000	3.6	3.7	2000	6.0	7.4	3000	4.2	6.7	2000	5.4	13.4
3000	4.9	3.6	2000	5.0	3.9	2000	4.1	3.9	2000	6.9	8.0	3000	5.3	7.2	2000	6.5	14.1
3000	5.9	4.1	2000	5.6	4.2	2000	4.7	4.2	2000	7.6	8.6	3000	6.3	7.9	3000	7.6	14.9
3000	6.5	4.5	2000	6.1	4.7	2000	5.3	4.6	2000	8.3	9.3	3000	7.5	8.9	3000	8.9	16.4
3000	7.5	5.3	2000	6.7	5.2	3000	6.1	5.1	2000	9.0	10.0	3000	8.6	10.3	2000	10.0	18.0
3000	8.2	6.1	2000	7.3	5.6	3000	6.9	5.6	2000	9.8	10.9	3000	9.7	11.8	2000	11.2	19.5
3000	9.0	6.9	2000	7.9	6.1	3000	7.8	6.4	2000	10.3	11.8	3000	10.8	13.7	1500	12.7	20.5
3000	10.0	7.6	2000	8.4	6.7	3000	8.5	7.3	2000	10.6	12.8	3000	11.7	16.1			
3000	10.8	8.3	3000	9.0	7.3	3000	9.7	8.4	2000	11.2	13.7	2000	12.7	18.0			
3000	11.6	9.7	3000	9.8	8.2	3000	10.6	9.3	2000	12.7	14.7						
3000	12.7	11.2	3000	10.9	9.5	3000	11.5	10.4									
			3000	12.1	10.9	2000	12.7	11.5									
			2000	12.7	11.8												

NOTE: All crack lengths are in mm.
All tests were terminated when "a" reached near surface of specimen.

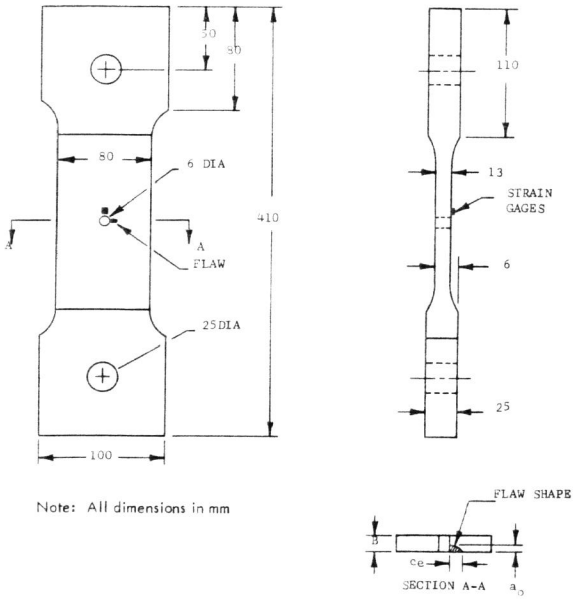

Figure 1 Test Specimen

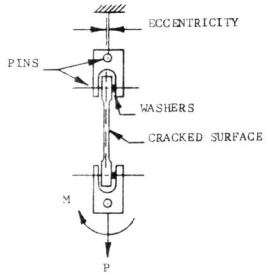

Figure 2 Combined Tension and Bending Test Arrangement

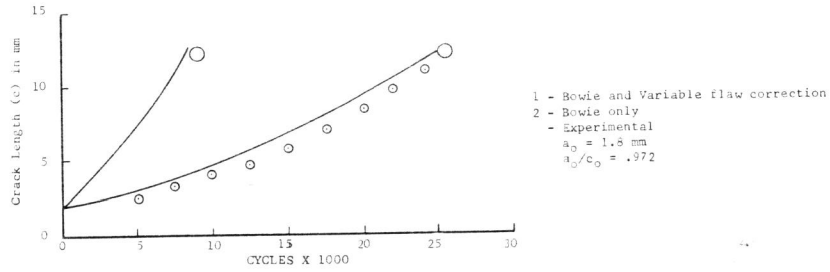

Figure 3 Crack Growth versus Number of Cycles Under Tension

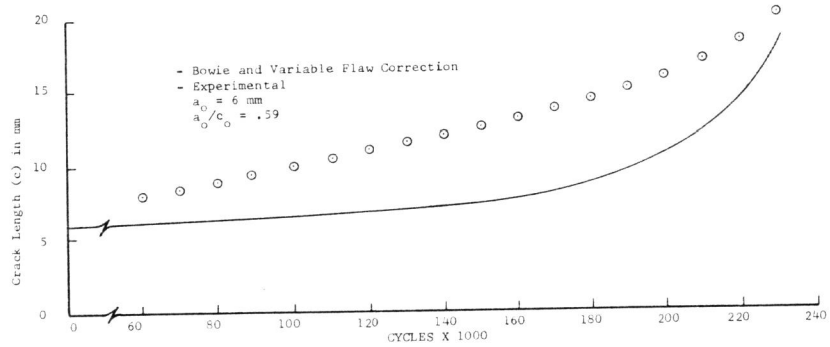

Figure 4 Crack Growth versus Number of Cycles Under Bending